ELSEVIER

Biochimica et Biophysica Acta 1609 (2003) 28–38

BIOCHIMICA ET BIOPHYSICA ACTA
BBA

www.bba-direct.com

Piracetam inhibits the lipid-destabilising effect of the amyloid peptide Aβ C-terminal fragment

Marie-Paule Mingeot-Leclercq[a,*], Laurence Lins[b], Mariam Bensliman[a], Annick Thomas[c], Françoise Van Bambeke[a], Jacques Peuvot[d], André Schanck[e], Robert Brasseur[b]

[a] *Unité de Pharmacologie Cellulaire et Moléculaire, Université catholique de Louvain, Avenue E. Mounier, 73. Bt 7370. B-1200 Brussels, Belgium*
[b] *Centre de Biophysique Moléculaire Numérique, Faculté Universitaire des Sciences Agronomiques, B-5030 Gembloux, Belgium*
[c] *INSERM 410, IFR X Bichat, 75018 Paris, France*
[d] *UCB Pharma, B-1420 Brainel'Alleud, Belgium*
[e] *Unité de Chimie Structurale et des Mécanismes Réactionnels, Université catholique de Louvain, B-1348 Louvain-La-Neuve, Belgium*

Received 6 August 2002; received in revised form 17 October 2002; accepted 5 November 2002

Abstract

Amyloid peptide (Aβ) is a 40/42-residue proteolytic fragment of a precursor protein (APP), implicated in the pathogenesis of Alzheimer's disease. The hypothesis that interactions between Aβ aggregates and neuronal membranes play an important role in toxicity has gained some acceptance. Previously, we showed that the C-terminal domain (e.g. amino acids 29–42) of Aβ induces membrane permeabilisation and fusion, an effect which is related to the appearance of non-bilayer structures. Conformational studies showed that this peptide has properties similar to those of the fusion peptide of viral proteins i.e. a tilted penetration into membranes. Since piracetam interacts with lipids and has beneficial effects on several symptoms of Alzheimer's disease, we investigated in model membranes the ability of piracetam to hinder the destabilising effect of the Aβ 29–42 peptide. Using fluorescence studies and ^{31}P and ^{2}H NMR spectroscopy, we have shown that piracetam was able to significantly decrease the fusogenic and destabilising effect of Aβ 29–42, in a concentration-dependent manner. While the peptide induced lipid disorganisation and subsequent negative curvature at the membrane–water interface, the conformational analysis showed that piracetam, when preincubated with lipids, coats the phospholipid headgroups. Calculations suggest that this prevents appearance of the peptide-induced curvature. In addition, insertion of molecules with an inverted cone shape, like piracetam, into the outer membrane leaflet should make the formation of such structures energetically less favourable and therefore decrease the likelihood of membrane fusion.

Keywords: Piracetam; Aβ 29–42 peptide; Membrane; Lipid; Liposome; Conformational analysis; Fusion; Permeability; NMR; Tilted peptide

1. Introduction

Alzheimer's disease is a progressive degenerative disease of the brain characterized by loss of cognitive function (dementia), selective neuronal death and abnormal formation in the brain of neuritic amyloid plaques. Genetic, neuropathologic, transgenic and modelling studies implicate the accumulation of β-amyloid peptides (Aβ) as an important step in the pathogenesis of the disease [1,2]. Aβ is a 40/42-residue proteolytic fragment of amyloid precursor protein (APP), an ubiquitous transmembrane protein [3]. Under pathological conditions, Aβ polymerises into extended β-sheet structures that result in Aβ fibrils characteristic of the amyloid plaque.

The mechanism leading to Aβ toxicity has been extensively debated [4,5]. The hypothesis that interactions between Aβ aggregates and neuronal membranes play an important role in toxicity is now generally accepted [6]. In vivo studies have shown that Aβ proteins aggregate in a membrane-bound conformation in dog and human brain sections [7,8] and induce free-radical oxidative stress of neuronal lipids in brain of Alzheimer patients [9]. In cellular models, Aβ has been reported to alter intramembranous structures [10], to increase permeability in lysosomal and endosomal vesicles [11], to induce the formation of cation-permeable channels [12] and to enhance the activity of phospholipases A_2, C and D [13–16]. In addition to these in vivo and cellular observations, numer-

* Corresponding author. Tel.: +32-2-764-73-74; fax: +32-2-764-73-73.
E-mail address: mingeot@facm.ucl.ac.be (M.-P. Mingeot-Leclercq).

0005-2736/02/$ - see front matter
PII: S0005-2736(02)00654-5

ous studies have been performed using models of membrane to characterise at the molecular level the binding of Aβ fragments to lipids [17–19], and the effects of this interaction on the biophysical properties of the membrane. In this respect, Aβ peptides induce liposome fusion [20], leakage of encapsulated dyes [17], formation of ion-channels [21,22] and perturbations in membrane fluidity [23–27].

Focusing on membrane destabilisation and on the C-terminal domain of Aβ (residues 29–40 and 29–42) which is critical for amyloid aggregation and fibril stabilisation [28,29], Brasseur [30] has related membrane destabilisation to the ability of the Aβ C-terminal fragment to penetrate into membranes with a 30–60° tilt with respect to the plane of the lipid/water interface.

A number of approaches have been investigated to improve the daily living activities of patients presenting Alzheimer's disease. For example, *Ginkgo biloba*, tacrine, donezepil (acetylcholinesterase inhibitors), nimodipine (calcium channel blocker) and piracetam (nootropic agent) have been approved for the treatment of demented patients in some European countries [31]. Clinical insights into nootroopic agents have shown that (i) long-term and high dose treatment with piracetam may slow down the progression of several clinical features of Alzheimer's disease [32], (ii) they have a comparable efficacy to acetylcholinesterase inhibitors [33] and (iii) the cognitive relapse after discontinuation of the drug therapy is less pronounced compared to cholinesterases inhibitors [34]. However, the molecular mechanism of piracetam's beneficial effects in Alzheimer's disease is not yet understood. Since results from the literature suggest that piracetam interacts with lipids [24], we have investigated in model membrane systems the ability of piracetam to hinder the membrane destabilising effect of the Aβ 29–42 synthetic peptide.

2. Materials and methods

2.1. Preparation of small unilamellar vesicles (SUV liposomes)

These studies were performed on SUV, made of phosphatidylcholine (PC)/phosphatidylethanolamine (PE)/phosphatidylinositol (PI)/phosphatidylserine (PS)/sphingomyelin (SM)/cholesterol (Chol) (30%:30%:2.5%:10%:5%:22.5%) to mimic to some extent the composition of the neuronal membrane [35].

A dry lipid film was obtained by evaporation of the solvents of lipids ($CHCl_3$/CH_3OH: 2:1) in a rotavapor. After overnight dessication, liposomes were prepared by 1-h hydration of the dry lipidic film with Tris buffer pH 8 (Tris 10 mM, NaCl 150 mM, EDTA 0.1 mM, NaN_3 1 mM) at 37 °C in a nitrogen atmosphere. The suspension was sonicated at 4 °C under a stream of nitrogen with a Braun Labsonic-L sonotrode (Braun Biotech International, Melsungen, Germany) set at 50 W for 5×2 min with 1-min cooling intervals until the opaque suspension became translucent. The preparations were then centrifuged at 1000 rpm for 10 min (Damon IEC–CRU-5000) to remove particulate matter. The actual phospholipid concentration of each preparation was determined by phosphorus assay [36]. Total lipid concentration was calculated assuming a similar recovery of phospholipids and cholesterol. Liposomes were used the day following their preparation.

2.2. Fluorescence and light scattering studies

2.2.1. Fusion of lipidic phase

The fusion of lipidic phases was determined by measuring the dequenching of the fluorescence of octadecylrhodamine B chloride (R_{18}) [37]. The fluorescence of this lipid-soluble probe is self-quenched in proportion with its membranous concentration and any decrease of its surface density is therefore associated with a commensurate increase of the fluorescence intensity of the preparation [37]. Labeled liposomes were obtained by incorporating R_{18} in the dry lipid film at a molar ratio of 5.7% with respect to the total lipids and diluted to a concentration of 5 μM in total lipids. These labeled liposomes were mixed with unlabeled liposomes (adjusted to the same concentration) at a ratio of 1:4. Peptide (or piracetam) were added and the fluorescence was thereafter followed at room temperature during 25 min, using λ_{exc} of 560 nm and λ_{em} of 590 nm (Perkin-Elmer LS-30, Perkin-Elmer Ltd, Beaconsfield, UK). Additional experiments were performed where liposomes were either preincubated 20 min with piracetam before the addition of peptides or with peptides during 20 min prior addition of the drug. Results were expressed as fluorescence values calculated as the difference between the fluorescence signal recorded for the mixing of labeled and unlabeled liposomes and that recorded in identical experimental conditions for the labeled liposomes mixed with peptide or piracetam. This correction was made to rule out any interference of the peptide or piracetam on the fluorescence of the marker.

2.2.2. Fusion of aqueous phase

Two preparations of labeled liposomes were used. The first population of liposomes contained hydroxypyrene-1,3,6-trisulfonic acid (HPTS; 1 mM) and the second *p*-xylene-bis-pyridinium bromide (DPX; 50 mM) dissolved in Tris buffer pH 8 (Tris 10 mM, NaCl 150 mM, EDTA 0.1 mM, NaN_3 1 mM). The mixture of aqueous phases of the two populations of liposomes was monitored by the decrease of HPTS fluorescence due to the quenching of HPTS fluorescence by DPX. After liposome preparations, the unentrapped probes were eliminated by minicolumn centrifugation. The two types of liposomes were diluted with Tris buffer pH 8 at 50 μM and mixed at a ratio of 1:1. Peptide (or piracetam) was added to the liposomes and the fluorescence was thereafter followed at room temperature during 25 min. In some experiments, liposomes were

preincubated 20 min with piracetam before the addition of peptide whereas in others, the drug was mixed to liposomes preincubated 20 min with peptide. Fluorescence of HPTS was monitored with a Perkin-Elmer LS30 fluorescence spectrophotometer (Perkin-Elmer) using λ_{exc} of 450 nm and λ_{em} of 512 nm.

2.2.3. Determination of the size of liposomes

The apparent average diameter of SUV was determined by quasi-elastic light scattering spectroscopy [38] using a Coulter® Nano Sizer™ N_4MD (Coulter Electronics Ltd, Luton, UK), as described earlier [39]. The liposomes concentration was set at 65 μM (total lipids).

Fluctuation of light scattering was measured at an angle of 90° with monodisperse latex particles of 100- and 800-nm diameters as control. Data were analyzed using size distribution analysis mode to determine the full size distribution profile of liposomes mixed with the β-amyloid peptide and/or piracetam. In some experiments, liposomes were preincubated 20 min with piracetam before the addition of peptide whereas in others the drug was mixed after incubation during 20 min of liposomes with peptide.

2.2.4. Permeability studies

As described by Weinstein et al. [40], leakage of entrapped, self-quenched calcein from liposomes can be monitored by the fluorescence increase subsequent to its dilution. The dried lipid films were hydrated with a solution of purified calcein (16.3 mM) which had an osmolarity of 461 mOsm/kg [measured by the freezing point technique (Advanced Instruments, Needham Heights, MA)]. After preparation of the vesicles, the unencapsulated dye was eliminated by the minicolumn centrifugation technique [41]. The liposomes were diluted to a final lipid concentration of 5 μM in an isoosmotic 231 mM Tris buffer pH 8 (461 mOsm/kg), and then the peptide (or piracetam) was added at room temperature. Again, additional experiments were performed with liposomes preincubated 20 min with piracetam (or peptide) before the addition of peptide (or piracetam). The percentage of calcein released under the influence of peptide was defined as $[(F_t - F_{contr})/(F_{tot} - F_{contr})] \times 100$, where F_t is the fluorescence signal measured at time t in the presence of the peptide, F_{contr} is the fluorescence signal measured at the same time t for control liposomes, and F_{tot} is the total fluorescence signal obtained after complete disruption of the liposomes by sonication (checked by quasi-elastic light spectroscopy). All fluorescence determinations were performed at room temperature on a Perkin Elmer LS 30 Fluorescence Spectrophotometer (Perkin-Elmer) using λ_{exc} of 472 nm and λ_{em} of 516 nm.

2.3. NMR studies

2.3.1. ^{31}P NMR

Multilamellar vesicles (MLV) of the same composition as that used for fluorescence and light scattering studies were prepared as follows: organic solutions of the lipids were dried under vacuum, hydrated over 1 h at 37 °C in Tris buffer pH 8 at a concentration of 10 mM in phospholipids, maintained at 37 °C for a further hour and finally submitted to five freeze–thawing cycles. The same procedure was used for preparing DMPC/DHPC (dimyristoylphosphatidylcholine/dihexanoylphosphatidycholine in a molar ratio of 3:2) liposomes at a concentration of 20 mM in phospholipids.

Peptide-containing samples were prepared by the following procedure: peptides were first dissolved in trifluoroacetic acid [42], the solvent removed with N_2 gas and the sample dried under vacuum. The peptide dissolved in DMSO (6 mg/ml) was simply added to the MLV suspension. Piracetam-containing samples were obtained by dissolving in the buffer the necessary amount of drug to reach a 200 mM final concentration in the sample.

^{31}P NMR spectra were obtained at 101.3 MHz with an AC 250 Bruker spectrometer. Two milliliters of MLV suspension were used in 10-mm NMR tubes. D_2O (15%) was added for locking on the deuterium signal. Fourier transform conditions were: 25 kHz spectral width, 4 K data points, flip angle 40° (10 μs), 1.2 s pulse interval. Five thousand scans were accumulated and a 50-Hz line broadening was applied to the free induction decay before Fourier transformation. Powergated ^1H decoupling was applied. Experiments were conducted as a function of temperature: samples were heated and cooled down with 30-min equilibration times between each accumulation at each new temperature.

2.3.2. ^2H NMR

Aqueous solution of binary mixtures of long- and short-chain phosphatidylcholines may form a well-oriented nematic phase of bilayered discoidal mixed micelles called bicelles [43]. We used DMPC/DHPC in a molar ratio of 3.5:1. The DMPC solution in $CHCl_3$ (containing 25% of DMPC-d_{54}) was evaporated under vacuum, resuspended in ^2H-depleted water and vortexed, centrifuged and freeze–thawed for obtaining a homogeneous slurry. Stock solution of DHPC in ^2H-depleted water was added to the DMPC suspension. The final phospholipid content of 20% (w/w) was adjusted with 50 mM 2-morpholinoethane sulfonic acid monohydrate (MES) pH 6.

Peptide-containing samples were prepared by the same procedure as for ^{31}P NMR studies but the Aβ 29–42 in DMSO (see supra) was added to a $CHCl_3$ solution of DMPC. The solvents were evaporated under vacuum, the dry peptide–DMPC mixture was resuspended in ^2H-depleted water and this suspension was treated as control samples (see above) before addition of DHPC solution and buffer. During this study, severe difficulties appeared in the bicelle preparation: the samples were highly viscous but not completely transparent. After centrifugation, the suspension became more transparent but a pellet was observed, indicating that the peptide was not well inserted

in the bicelles. For improving this incorporation, we decided to perform the ^{2}H NMR study with a less hydrophobic fragment of Aβ, the 22–42 peptide. This fragment, which also induces significant lipid fusion [20], is much less hydrophobic than the Aβ 29–42 as indicated by the calculated grand average of hydrophobicity (GRAVY index; [44]) (1.07 vs. 2.41) or by the normalised consensus hydrophobicity scale of Eisenberg et al. [45] (0.47 vs. 0.89). We decided to synthesise this fragment with a Tyr residue at the N-terminus (GRAVY index of 0.96) to allow the peptide purification by HPLC.

The incorporation of Tyr-22–42 in bicelle solutions was satisfactory. The longer peptide-containing samples were transparent and highly viscous after addition in DHPC solution.

The preparation of piracetam-containing samples was similar to that of control bicelles, but the drug was dissolved in the ^{2}H-depleted water employed for resuspending DMPC or DMPC–peptide mixture.

NMR samples of 200 μl were introduced in short 5-mm tubes and sealed tightly. Before data acquisition, the samples were kept a 37 °C for 1 h, for allowing equilibrium alignment to be established. Deuterium NMR spectra were recorded at 55.3 MHz on a Chemagnetics CMX 250/360 spectrometer. The standard quadruple echo sequence [46] with $\tau = 50$ μs, 90° pulse of 2.1 μs and a repetition time of 1.2 s was used. Four thousand scans were accumulated; 4 K data points were acquired, fractionally left-shifted to start the record at the top of the echo, baseline-corrected and zero-filled to 16 K. A line broadening of 100 Hz was applied to the free induction decay prior to Fourier transformation.

2.4. Computational methods

2.4.1. 3D construction of the molecules

3D structure of peptides, phospholipids and piracetam was calculated as previously described [20,47–49]. The methods account for the contribution of a lipid–water interface by the concomitant variation of the dielectric constant and the energy of transfer of atoms from a hydrophobic to a hydrophilic environment.

For the Aβ Tyr-22–42 peptide, the conformation of the 22–28 segment was calculated using the stereoalphabet procedure [50,51], with the 29–42 end considered as α-helical. Briefly, in this procedure, six values of ϕ/ψ torsional angles (ϕ and ψ values: $-60, -40$; $-160, +160$; $-140, +80$; $-80, +160$; $-80, +80$; $+60, +60$), representing the most frequent angle pairs of the Ramachandran plot, are combined to find the most stable conformation of the whole Aβ Tyr-22–42 peptide. 6^n conformations of the peptide are thus considered, with $n = 7$ (residues 22 to 28). The most stable structure after energy minimisation is considered for further calculations.

The molecules were then oriented at the hydrophobic/hydrophilic interface taking into account the hydrophobic and hydrophilic centres, calculated as described elsewhere [47].

The molecular hydrophobicity potential (MHP) of piracetam was determined as described by Brasseur [48].

2.4.2. Assembly of Aβ Tyr-22–42 or Aβ 29–42 with phospholipids and piracetam

The procedure is derived from that used to surround drugs with lipids [47]. In the hypermatrix procedure, the lipid/water interface is taken into account by linearly varying the dielectric constant ε between 3 (above the interface) and 30 (below the interface).

In the calculations, we simulate the interaction of Aβ 29–42 or Aβ Tyr-22–42 with either dipalmitoylphosphatidylethanolamine (DPPE) molecules or with a lipid molecule (DPPE) complexed to piracetam. This complex was obtained as described previously [49].

The initial position and orientation of the molecules are defined using the TAMMO procedure [47]. The position of Aβ 29–42 or Aβ Tyr-22–42 is constant while the first lipid molecule (or lipid/piracetam complex) translates towards the peptide along the X axis by l steps of 0.05 nm. It rotates by steps of 30° around its Z' axis and around the X axis: l is the number of positions tested along the X axis, m is the number of rotations around the peptide and n is the number of rotations around the lipid (or lipid/piracetam complex) itself. For each set of l, m and n values, the energy of interaction between Aβ Tyr-22–42 (or Aβ 29–42) and lipid (or lipid/piracetam complex) is calculated as the sum of van der Waals, electrostatic and hydrophobic terms. Then, for each set of values l, m and n, the lipid (or lipid/piracetam) molecule moves by step of 0.05 nm along the Z' axis perpendicular to the interface and the angle of Z' axis bends $\pm 5°$ with respect to the Z axis. The energy values together with the coordinates of all assemblies are stored in a matrix and classified according to decreasing values. The most stable matching is used to decide the position of the first lipid (or lipid/piracetam complex). The position of the second lipid (or lipid/piracetam) is then defined as the next most energetically favourable orientation stored in the hypermatrix taking sterical and energetic constraints due to the presence of the first lipid molecule (or lipid/piracetam) taken into account. To further minimise the energy of the complex, the position of both lipid (or lipid/piracetam) molecules is alternatively modified according to the energy classification of the Hypermatrix. For the next lipid molecule, the same process is repeated but the positions of all surrounding molecules are modified alternatively in order to find the lowest energy state. In these calculations, the energy of interaction between all lipids is minimised. The process ends when Aβ Tyr-22–42 or Aβ 29–42 is completely surrounded with lipids (or lipid/piracetam complexes).

All calculations are performed on Pentium III processors, using the Z-TAMMO software. Graphs were drawn using Win-MGM (Ab Initio technology, Obernai, France).

2.5. Materials

Aβ 29–42 peptide was synthesised by Polypeptides laboratories (Wolfenbüttel, Germany) and solubilised in 1,1,1,3,3,3-hexafluoro-2-propanol (HFP) except for NMR measurements (cf. supra). The sequence of Aβ 29–42 is Gly-Ala-Ile-Ile-Gly-Leu-Met-Val-Gly-Gly-Val-Val-Ile-Ala. The synthesis of Aβ Tyr-22–42 fragment was performed by using FMOC chemistry on a PerSeptive Biosystem solid-state peptide synthesiser. The peptide was purified by HPLC (Waters) and its identity and purity were confirmed with mass spectrometry. Piracetam provided by UCB Pharma (Brainel'Alleud, Belgium) was solubilized in Tris buffer pH 8 or ^{2}H-depleted water for NMR measurements on bicelles. Egg yolk phosphatidylcholine, wheat germ phosphatidylinositol and egg yolk phosphatidylethanolamine (grade 1) were purchased from Lipid Products (Nr Redhill, UK). Sphingomyelin and cholesterol were obtained from Sigma Chemical Co. (St. Louis, MO). Bovine spinal cord phosphatidylserine was purchased from Avanti Polar Lipids, Inc. (Birmingham, AL). Octadecylrhodamine B (R18), hydroxypyrene-1,3,6-trisulfonic acid (HPTS) and *p*-xylene-bis-pyridinium bromide (DPX) were obtained from Molecular Probes (Eugene, OR, USA). Calcein, purchased from the Sigma Chemical Co., was purified by chromatography on Sephadex LH-20 following the technique of Lelkes [41], and the purity of the final product was checked by TLC on silica gel G using CH_3OH/NH_4OH 28% (9:1.5 v/v) as mobile phase. 1,2-Dimyristoyl-*n*-glycero-3-phosphocholine (DMPC), deuterated 1,2-di[myristoyl-d_{27}]-*n*-glycero-3-phosphocholine (DMPC-d_{54}) and 1,2-dihexanoyl-*n*-glycero-3-phosphocholine (DHPC) were purchased from Avanti Polar Lipids (Alabaster, AL) and deuterium [^{2}H]-depleted water from Cambridge Isotopes (Cambridge, MA). Other reagents were obtained from E. Merck (Darmstadt, Germany) and were of analytical grade.

3. Results

3.1. Fluorescence and light scattering studies

3.1.1. Fusion of lipidic phases

The measurement of fluorescence dequenching of octadecylrhodamine B (R_{18}) is an established technique to study the fast mixing of lipids occurring during fusion of adjacent membranes [37].

Piracetam did not induce any significant dilution of octadecylrhodamine B up to a piracetam/lipid molar ratio of 9600 during an exposure time of 25 min, suggesting no effect on mixture of lipidic phases (Fig. 1). In contrast, with peptide Aβ 29–42, a rapid and marked increase in fluorescence was observed over the first few minutes followed by a very slow increment, as already observed for other fusion peptides [20,52] (Fig. 1). The effect of peptide Aβ 29–42 was dose-dependent and was maximal for a peptide/lipid molar ratio of 0.2.

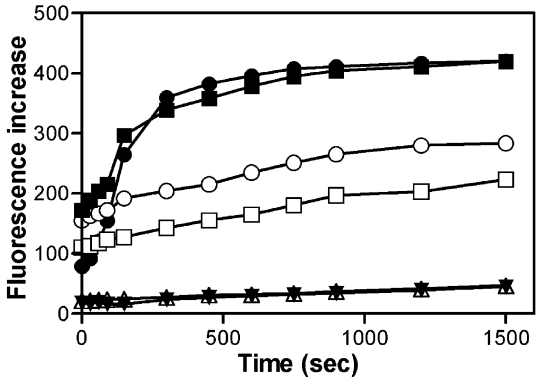

Fig. 1. Effect of piracetam and/or peptide Aβ 29–42 on the fusion of lipidic phases of liposomes. Liposomes (PC/PE/PI/PS/SM/Chol; 30%:30%:2.5%:10%:5%:22.5%) are added at room temperature to Aβ 29–42 (peptide/lipid molar ratio = 0.2) (■) or piracetam (piracetam/lipids = 9600) (▼). Piracetam was also first preincubated with liposomes during 20 min before addition of HFP or peptide at different piracetam/peptide ratios [(○) piracetam/peptide molar ratio = 9.6; (□) piracetam/peptide molar ratio = 96; (△) piracetam/peptide ratio = 960]. In additional experiments, piracetam was added after incubation of liposomes with peptide during 20 min (piracetam/peptide ratio = 960) (●). Each point is the mean value of three independent experiments but the S.D. (< 5) are not shown for the sake of clarity.

This increase of fluorescence induced by peptide was almost completely prevented when liposomes are preincubated with piracetam (20 min), before the addition of peptide (Fig. 1). This effect was concentration-dependent (increasing piracetam/peptide molar ratios from 9.6 to 960) and was not observed when piracetam was added after the incubation of liposomes with peptide.

3.1.2. Fusion of aqueous phases

Fusion of liposome aqueous compartments can be monitored by the decrease of HPTS fluorescence following the mixture of HPTS and DPX contained in the aqueous compartment of two separate liposome preparations.

Piracetam did not induce any significant decrease of fluorescence (up to a piracetam/lipid ratio of 9600) during an exposure time of 25 min (Fig. 2). In contrast, Aβ 29–42 induces a fast decrease of fluorescence ($t_{1/2} < 30$ s) which was peptide/lipid ratio-dependent (from a ratio of 0.3 to 3) (Fig. 2). The maximum effect was obtained at a peptide/lipid molar ratio of 3.

At this ratio, we investigated the effect of increasing amounts of piracetam (piracetam to peptide molar ratios from 9.6 to 960). Preincubation of piracetam, at a piracetam/peptide ratio of 960, during 20 min before the addition of peptide prevented almost completely the mixture of the two fluorescent probes. Again, it is interesting to note the dose-dependent effect and the fact that piracetam was not able to reverse the effect of the Aβ-amyloid fragment when peptide was first incubated with liposomes (Fig. 2).

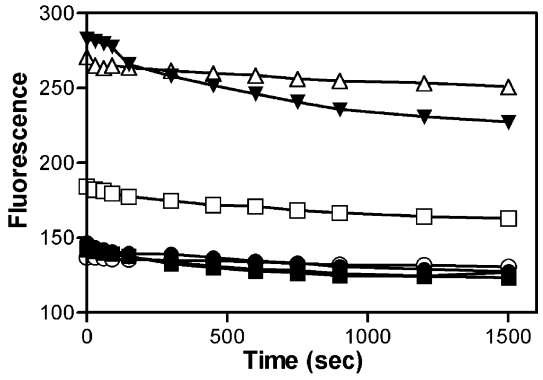

Fig. 2. Effect of piracetam and/or peptide Aβ 29–42 on the fusion of aqueous phases of liposomes. Liposomes (PC/PE/PI/PS/SM/Chol; 30%:30%:2.5%:10%:5%:22.5%) are mixed at room temperature with Aβ 29–42 (peptide/lipid molar ratio = 3) (■) or with piracetam (▼) (piracetam/lipids = 9600). Piracetam was also first preincubated 20 min with liposomes before addition of HFP or peptide at different piracetam/peptide ratios [(○) piracetam/peptide molar ratio = 9.6; (□) piracetam/peptide molar ratio = 96; (△) piracetam/peptide ratio = 960]. In additional experiments, piracetam was added after incubation during 20 min of liposomes with peptide (piracetam/peptide ratio = 960) (●). Each point is the mean value of three independent experiments but the S.D. (< 15) are not shown for the sake of clarity.

3.1.3. Size of the liposomes

To further verify the ability of Aβ 29–42 peptide and/or piracetam to induce fusion of membranes, we investigated their capacity to modify the apparent size and homogeneity of the liposomes preparation by means of a light scattering assay (Fig. 3).

Piracetam had no effect on the apparent size diameter of liposomes since the size obtained was similar to that observed for control liposomes. In contrast, at a peptide/lipid molar ratio of 2, Aβ 29–42 peptide caused a striking increase in the apparent diameter of the particles and induced the appearance of two populations (Fig. 3).

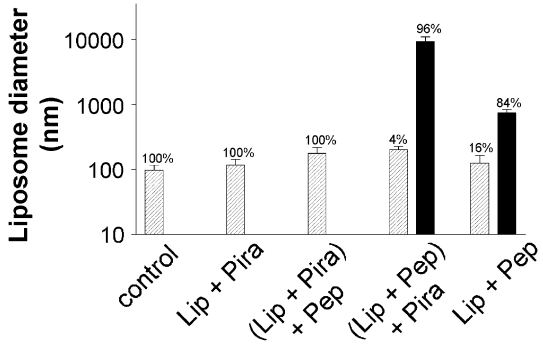

Fig. 3. Effect of piracetam and/or peptide Aβ 29–42 on apparent mean diameter of liposomes. Liposomes (PC/PE/PI/PS/SM/Chol; 30%:30%:2.5%:10%:5%:22.5%) are mixed at room temperature with Aβ 29–42 (peptide/lipid molar ratio = 2) or with piracetam (piracetam/lipid ratio = 19200). Piracetam was also first preincubated 20 min with liposomes before addition of HFP or peptide or added after incubation during 20 min of liposomes with peptide. The percentage of each population found is indicated at the top of the histogram. Readings are given as mean ± S.D.

Again, preincubation of liposomes with piracetam before the addition of peptide prevented the appearance of the two populations induced by the addition of peptide. As for the other experiments, no effect of piracetam was observed when the peptide was incubated with liposomes before the addition of the drug (Fig. 3).

3.1.4. Calcein permeability

Calcein is a polar molecule that has been widely used to study the permeability of lipid bilayers and has been originally described for this application by Weinstein et al. [40].

The effect induced by Aβ 29–42 peptide, piracetam or both on membrane permeability is shown on Fig. 4. In contrast to piracetam which did not induce any significant leakage of entrapped calcein (up to a piracetam/lipid ratio of 9600) during an exposure time of 25 min, Aβ 29–42 peptide induced a fast (< 60 s), dose-dependent and almost complete release of calcein from liposomes as observed previously for mellitin [53], a known porogenic agent [54]. The release was observed at peptide to lipid ratios ranging from 0.3 to 12 and was maximal from a ratio of 6.

At this peptide/lipid ratio, preincubation of piracetam with lipids prevented almost completely the release of calcein induced by the peptide in a dose-dependent fashion (piracetam/peptide ratios from 9.6 to 960). Again, piracetam was not able to reverse the effect of the Aβ-amyloid fragment when the peptide was incubated with liposomes prior to the addition of piracetam (Fig. 4).

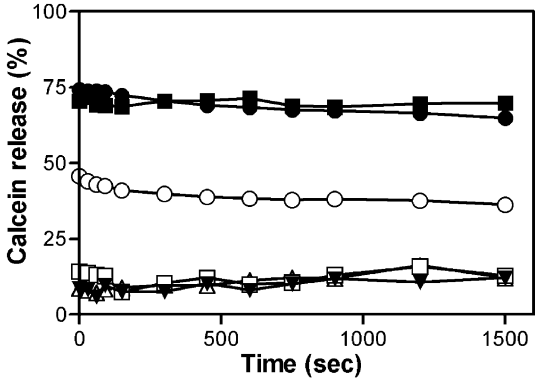

Fig. 4. Effect of piracetam and/or peptide Aβ 29–42 on the calcein release from liposomes. Liposomes (PC/PE/PI/PS/SM/Chol; 30%:30%:2.5%:10%:5%:22.5%) are added at room temperature to Aβ 29–42 (peptide/lipid molar ratio = 6) (■) or piracetam (▼) (piracetam/lipids = 9600). Piracetam was also first preincubated 20 min with liposomes before addition of HFP or peptide at different piracetam/peptide ratios [(○) piracetam/peptide molar ratio = 9.6; (□) piracetam/peptide molar ratio = 96; (△) piracetam/peptide ratio = 960]. In additional experiments, piracetam was added after incubation during 20 min of liposomes with peptide (piracetam/peptide ratio = 960) (●). Each point is the mean value of three independent experiments but the S.D. (< 2.5%) are not shown for the sake of clarity.

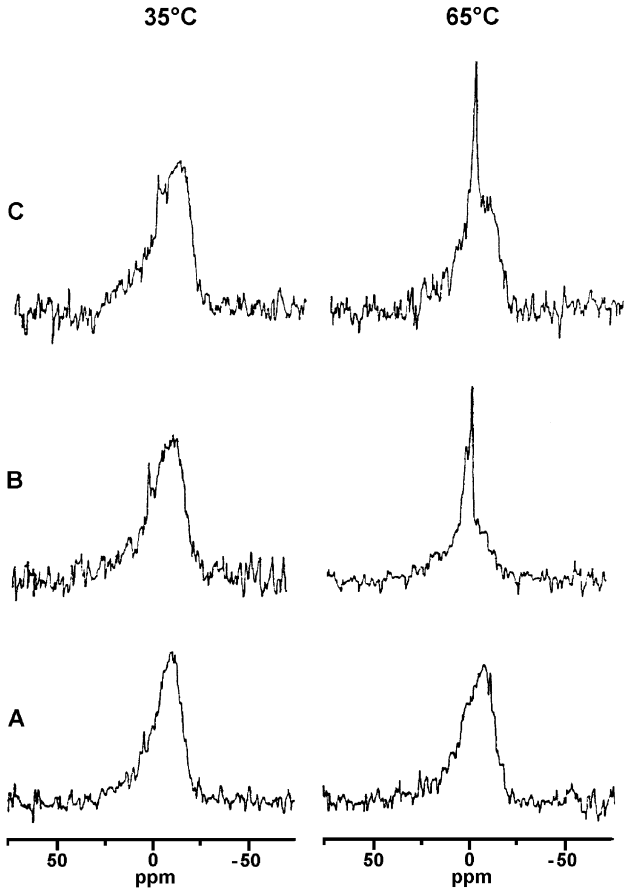

Fig. 5. ^{31}P NMR spectra of multilamellar liposomes upon warming (35 and 65 °C). (A) Control liposomes (PC/PE/PI/PS/SM/Chol; 30%:30%:2.5%:10%:5%:22.5%); (B) After addition of Aβ 29–42 (peptide/phospholipids 0.2); (C) with preliminary addition of piracetam (200 mM) and subsequent addition of Aβ 29–42 peptide (peptide/phospholipids 0.2).

3.2. NMR studies

3.2.1. ^{31}P NMR

Spectra were recorded for control liposomes and samples containing either Aβ 29–42 or piracetam and peptide. Typical spectra are shown on Fig. 5. Control liposomes (Fig. 5A) gave a broad spectrum characteristic of MLV with a maximum at high field and a shoulder at low field. At peptide/phospholipid ratio of 0.2, peptide-containing liposomes spectra (Fig. 5B) revealed modifications of lipid organisation depicted by a narrow signal that became very important at 65 °C. Addition of piracetam in liposome suspension (drug/lipid ratio of 20) had no significant influence on the spectral shapes (data not shown) but incubation of liposomes with piracetam prior to the addition of the peptide to the sample markedly reduced the peptide effect as illustrated by the reduction of the narrow signal at 65 °C (Fig. 5C) compared to what was observed for MLV incubated with peptide alone (Fig. 5B). The Aβ 29–42 peptide effect was irreversible since adding piracetam to peptide-containing liposomes had no influence on the development of the narrow signal induced by the peptide (data not shown).

For comparing the effect of Aβ 29–42 fragment with that of peptide Aβ Tyr-22–42 which was used in the ^{2}H NMR studies performed with DMPC/DHPC bicelles, ^{31}P NMR spectra of DMPC/DHPC (3:2 molar ratio) liposomes were run without and with that longer peptide. Control liposomes (Fig. 6A) revealed a small proportion of narrow peak that increased when Tyr-22–42 peptide was added to the liposomes (peptide/phospholipids ratio of 0.04) (Fig. 6B). Since after purification of Aβ Tyr-22–42 fragment a very limited amount of peptide was obtained, all the available peptide was used for ^{2}H NMR measurements on bicelle samples.

3.2.2. ^{2}H NMR

The ^{2}H quadruple echo spectrum of DMPC-d_{54} in bicelles was run for control sample (Fig. 7A). The deuteron spectra are characteristic of macroscopically aligned phospholipid bilayers oriented with their normal orthogonal to the magnetic field direction [43]. The 90° components of the ^{2}H powder pattern are the only visible components for this sample with a very high degree of orientation. The separation between the outermost lines corresponds to the quadrupolar splitting of the C_2–C_5 methylene groups of DMPC (plateau region) while the central doublet is assigned to the deuteron resonance of the DMPC terminal methyl group [55].

The incorporation of piracetam in bicelle solution slightly modified the ^{2}H NMR spectrum of DMPC-d_{54} in bicelles. As seen on spectra of Fig. 7B, the resolution of spectral components is reduced compared to that observed for control bicelles. The temperature effect between 35 and 40 °C was negligibly small.

The incorporation of Aβ Tyr-22–42 peptide in the bicelle preparation had dramatic effects on the spectral shape (Fig. 7C). Already at 35 °C, the broadening of the spectral components evidenced phospholipid structural perturbation. By heating the sample up to 40 °C, a narrow peak became prominent and this transformation became more pronounced even after cooling the sample down to 35 °C.

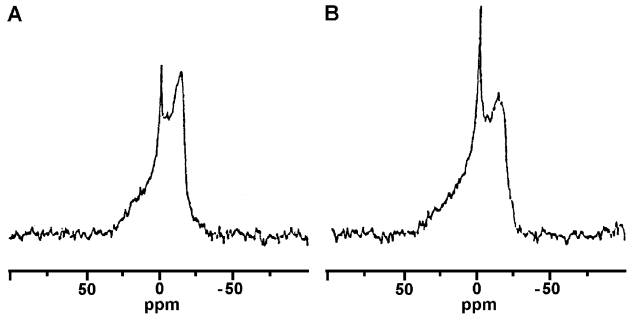

Fig. 6. ^{31}P NMR spectra at 25 °C of DMPC/DHPC (3:2 molar ratio) multilamellar liposomes after a thermal cycle (heating from 25 to 45 °C and cooling down to 25 °C). (A) Control liposomes; (B) After addition of Tyr-22–42 fragment (peptide/phospholipids 0.04).

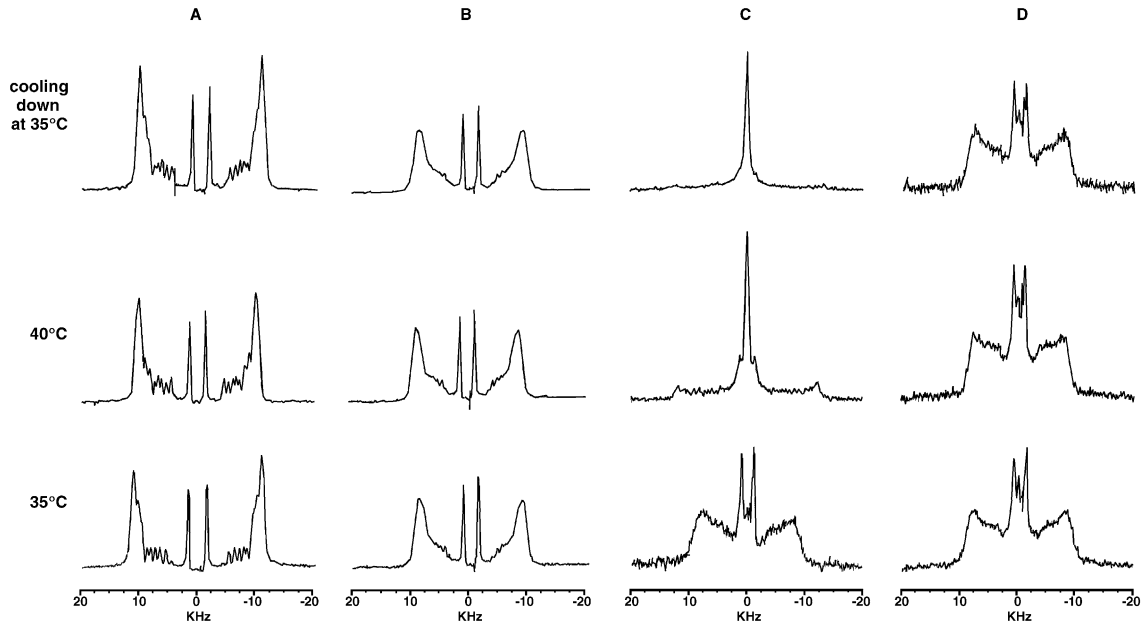

Fig. 7. ^{2}H NMR spectra of DMPC-d_{54} in DMPC/DHPC (3.5:1) bicelle solution at 35 and 40 °C and after cooling down at 35 °C. (A) Control bicelles; (B) Piracetam (200 mM) containing DMPC/DHPC bicelle solution; (C) Tyr-22–42 peptide containing bicelles (peptide/phospholipids 0.04); (D) Piracetam (200 mM) containing DMPC/DHPC bicelle solution submitted to the Tyr-22–42 peptide action (peptide/phospholipids 0.04).

In the presence of preliminary added drug and subsequent addition of Aβ Tyr-22–42 fragment (Fig. 7D), the major spectral modification at 35 °C induced by the peptide was prevented. Raising and lowering temperature did not appreciably modify the spectral line shape.

As observed by ^{31}P NMR, when piracetam was added to the peptide-containing bicellar sample, the spectrum evolution was similar to that observed on sample containing only the peptide (data not shown). The transformations induced by the peptide are irreversible.

3.3. Molecular modelling

The molecular structure of piracetam is presented on Fig. 8A; it was obtained as described elsewhere [49]. Molecular Hydrophobicity Potentials (MHP) (Fig. 8B), based on atomic transfer energies and calculated as described by Brasseur [48], show clearly that piracetam is perfectly amphipathic, one moiety being hydrophilic (green envelope) and the other being hydrophobic (orange envelope). This property is related to the ability of piracetam to coat the phospholipid headgroups [49].

The interaction between the Aβ Tyr-22–42 peptide and DPPE molecules was calculated using the hypermatrix procedure [47]. Fig. 9A shows clearly that the peptide induces a destabilisation of the lipids by disturbing the parallelism of the acyl chains. This is accompanied by the appearance of a negative curvature at the lipid surface. As already suggested for other tilted peptides [30], these changes could be the first events leading to lipid fusion. In contrast, when the same peptide interacts with DPPE in the

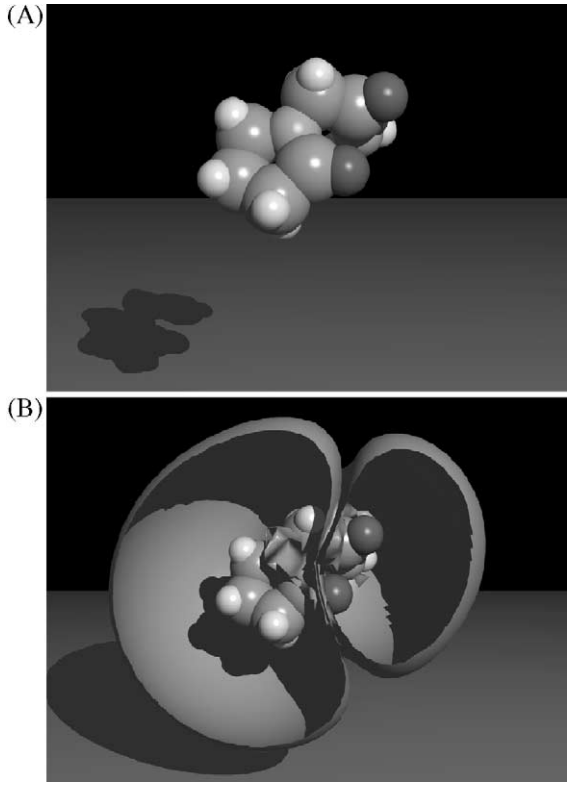

Fig. 8. (A) CPK (Corey-Pauling-Kaltum) representation of piracetam. Color of atoms is as follows: grey:carbon; blue:nitrogen; red:oxygen; white:-hydrogen; (B) MHP surfaces (calculated as described by Brasseur [48]) around piracetam in the same orientation as in (A). Green surface represents the hydrophilic domain, and the orange surface the hydrophobic one. The surfaces are cut by a plane to visualize the molecule.

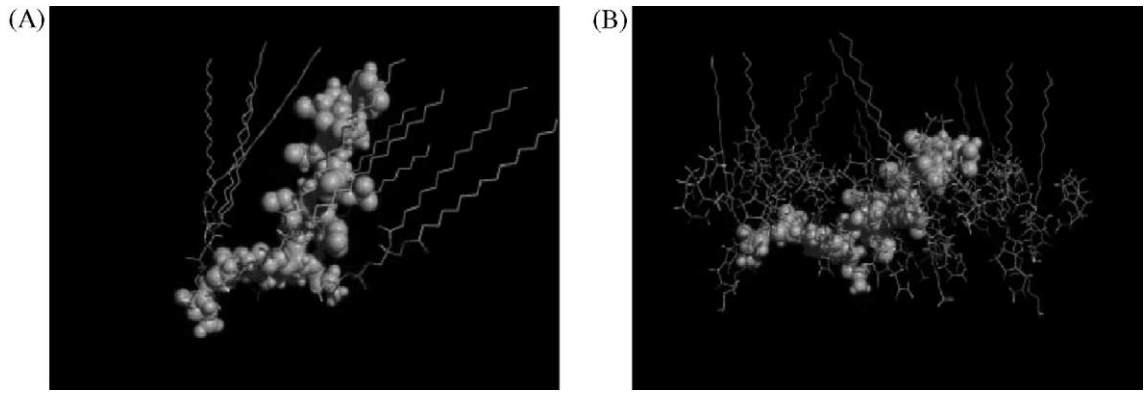

Fig. 9. (A) interaction between the Aβ Tyr-22–42 peptide (green CPK representation) and DPPE lipid molecules. Assembly is calculated as described in Section 2. The yellow lines indicate the tilt of the acyl chains induced by the peptide. The dashed yellow curve indicates the effect on the lipid curvature; (B) same as in (A) for the interaction between the Aβ Tyr-22–42 peptide, DPPE and piracetam.

presence of piracetam, these effects are lost, i.e. no perturbation of the acyl chain organisation can be observed, as well as no change in the lipid curvature (Fig. 9B). The same was observed when calculating the interaction of Aβ 29–42 with DPPE and DPPE/piracetam complexes (data not shown).

4. Discussion

The development of new therapeutic approaches to the treatment of cognitive disorders is a real and urgent problem due to demographic changes and the strong increase in mean life expectancy in developed countries. Among the possible therapeutic interventions, 2-pyrrolidone derivatives [56] such as piracetam are currently used in some countries. This nootropic agent for which no metabolite has been found [57] is known to enhance the oxidative glycolysis, to increase acetylcholine release and synthesis of cytochrome *h5* [58], to improve red blood cell deformability in vitro and to restore impaired deformability of physiologically deoxygenated sickled red cells [59]. In addition, recent interest has focused on the neuroprotective effects of piracetam, for instance, in the aftermath of acute stroke [60] and on its antimyoclonic action [61]. The molecular basis of piracetam beneficial effects in Alzheimer's disease is, however, unknown.

By using biophysical techniques, NMR spectroscopy and conformational analysis, the present study was aimed at investigating the effect of piracetam on the lipid-destabilising activity induced by Aβ fragments. The in vivo relevance of the experimental model employed in the current work has been ascertained by literature data. With respect to peptides, most of our experiments were carried out with Aβ 29–42 at peptide concentrations varying from 1 to 50 μM. Under normal conditions the physiological concentration of Aβ in the cerebrospinal fluid is around 0.5 nM [62,63] but by aging or under pathological situations, the degradation pathway of Aβ via the low density lipoprotein receptor-related protein or via a scavenger receptor is reduced by ~ 45% [64], which would increase the extracellular content of Aβ. Moreover, since biological membranes are heterogeneous, locally high peptide concentrations can be obtained transiently and, thus, the peptide concentrations used could be similar to those found under in vivo conditions. Likewise, the maximum effect of piracetam was observed for drug concentrations compatible with those used in clinics (piracetam/peptide ratio of ~ 1000 implying a piracetam concentration of 10 mM; [65]).

One of the most characteristic neuropathological signs of Alzheimer's disease is the deposition of neuritic plaques composed of Aβ proteins, 39–42 amino acids long, and derived from the transmembrane region of the APP [66]. Conformational analysis of the Aβ protein showed that its C-terminal domain (e.g. amino acids 29–40 or 29–42) has properties similar to those of the fusion peptide of viral proteins [67], i.e. a tilted penetration into membranes [48,52]. This oblique insertion is thought to be responsible for disturbance of the acyl chain parallelism, curvature of the membrane surface and, consequently, membrane destabilisation. As previously shown [20,68], Aβ 29–42 or its less hydrophobic analog Aβ 22–42 is able to induce membrane fusion and permeabilisation of lipid vesicles mimicking the composition of neuronal membranes [35]. We have shown here that the fusogenic effect is related to the appearance of non-bilayer structures where isotropic motion occurs, as measured by ^{31}P NMR studies, an observation which was previously related to fusogenic properties of other peptides [69–72]. As observed by ^{2}H NMR, the Aβ Tyr-22–42 fragment effect on bicelles [73,74] is quite comparable to the 29–42 fragment perturbing effect. Aβ Tyr-22–42 disorganises the bilayer structure as seen on the spectra by the transformation of the broad signal into a relatively narrow peak. Molecular modelling calculations support these experimental observations and suggest that lipid destabilisation could be due to the ability of tilted peptides to adopt metastable positions in the presence of lipids [75].

According to several observations, emerging hypotheses to explain the benefit of piracetam in Alzheimer's disease may involve lipids. First, piracetam is an amphiphilic drug and several molecules of piracetam simultaneously interact with one phospholipid molecule, as shown by molecular modeling. In the case of DPPE, we can consider that more than 80% of the water molecules in contact with the phospholipid polar heads have been replaced by piracetam, thus modifying the physical properties of the phospholipids [24,49]. Second, using a two-hybrid system as described by Hughes et al. [76] and Festy et al. [77], we showed no effect of piracetam on the interaction properties of the entire Aβ protein. Third, in ^{1}H NMR, the proton chemical shifts of the drug mixed with Aβ 29–42 (2:1) obtained in organic solution did not reveal any significant modifications compared to the shifts of the drug alone in DMSO solution.

Investigating further the effect of piracetam on membrane fusion or permeability induced by Aβ peptide, we have shown that piracetam is able to significantly decrease the fusogenic and destabilising effect of Aβ 29–42, in a concentration-dependent manner. It is worth noting that the same is observed for Aβ 29–40 and Aβ 22–42. This is in agreement with the ^{31}P and ^{2}H NMR results since the phospholipid bilayer disorganisation induced by the two fragments and shown by the development of a narrow peak is substantially reduced in piracetam containing samples. This may be interpreted as a stabilisation of the bilayer structures that inhibits their transformation into isotropic structures responsible for the observed narrow signals as it was observed for inhibitors of viral fusion (lipogastrins [78]). This effect only occurs when the drug is incubated with liposomes prior to peptide addition. Adding piracetam to liposomes preincubated with peptide does not reverse the effect of the peptide on the lipids, suggesting that the lipid destabilising process induced by the peptide is irreversible.

According to our observations and data reported in the literature, the benefit of piracetam in Alzheimer's disease may thus result from interactions with lipids. Two main hypotheses could explain the potential inhibitory effect of piracetam on membrane destabilisation induced by Aβ 29–42. First, piracetam could make the membrane interfaces more polar and hydrated [79] and it is well known that strongly hydrated lipids such as phosphatidylcholine inhibit the fusion of viral membranes with negatively-charged liposomes [80,81]. Conversely, less hydrated lipids such as phosphatidylethanolamine sustain membrane destabilisation. Second, inhibition of fusion could also result from expanding the headgroup area of the outer monolayer so as to produce positive curvature strain, a process which locally curves the cell membrane in a direction opposite to that induced by the fusogenic peptide [82].

While the peptide induces lipid disorganisation and negative curvature of the membrane interface, conformational analysis showed that piracetam, when preincubated with lipids, coats the phospholipid headgroups. Calculations suggest that this prevents the appearance of curvature. This is especially pronounced for phosphatidylethanolamine. Additionally, insertion of molecules with an inverted cone shape, such as piracetam, into the outer leaflet of one or both membranes makes the formation of these structures energetically less favourable and therefore decreases the likelihood of membrane fusion. In such a manner piracetam may hinder the permeabilising effect of Aβ-peptide.

Taken together, our data indicate that piracetam inhibits the lipid-destabilising effect of the amyloid peptide, but additional knowledge on this protective effect is required to fully develop the therapeutic potential of 2-pyrrolidone derivatives.

Acknowledgements

R.B. is *Directeur de Recherche*, M.-P.M.-L. is *Maître de Recherche* and F.V.B. and L.L. are *Chercheurs Qualifiés* of the Belgian *Fonds National de la Recherche Scientifique*. This work was supported by the Belgian *Fonds de la Recherche Scientifique Médicale* (Grants 3.4589.96 and 3.4546.02 to M.-P.M.-L. and grant 9.4506.99 to A.S.), by the *Fonds Speciaux de Recherche* (FSR 2002) of the *Université catholique de Louvain* to M.-P.M.-L. and F.VB. and by *Region wallonne* (Grant 115020 to M.-P.M.-L. and R.B.). We wish to thank deceased Professor R.R. Vold for her hospitality and fruitful discussions. ^{2}H NMR measurements were performed in her laboratory by one of us (A.S.) during his sabbatical at UCSD (University of California, San Diego). We thank F. Andries-Renoird, M.C. Cambier, N. Aguilera and C. Flore for dedicated technical assistance, and Dr. Roy Massingham for the critical reading of the manuscript. The financial support of UCB Pharma is also gratefully acknowledged.

References

[1] D.J. Selkoe, Science 275 (1997) 630–631.
[2] D.J. Selkoe, Clin. Neurosc. Res. 1 (2001) 91–103.
[3] J. Hardy, Proc. Natl. Acad. Sci. U. S. A. 94 (1997) 2095–2097.
[4] L.L. Iversen, R.J. Mortishire-Smith, S.J. Pollack, M.S. Shearman, Biochem. J. 311 (1995) 1–16.
[5] M.P. Mattson, Q. Guo, K. Furukawa, W.A. Pedersen, J. Neurochem. 70 (1998) 1–14.
[6] J.N. Kanfer, G. Sorrentino, D.S. Sitar, Neurochem. Res. 24 (1999) 1621–1630.
[7] R.E. Torp, E. Head, C.W. Cotman, Prog. Neuro-Psychopharmacol. Biol. Psychiatry 24 (2000) 801–810.
[8] H. Yamaguchi, M.L.C. Maat-Schieman, S.G. van Duinen, F.A. Prins, P. Neeskens, R. Natte, R.A.C. Roos, J. Neuropathol. Exp. Neurol. 59 (2000) 723–732.
[9] D.A. Butterfield, J. Drake, C. Pocernich, A. Castegna, Trends Mol. Med. 7 (2001) 548–554.
[10] N.J. Lane, A. Balbo, R. Fukuyama, S.I. Rapoport, Z. Galdzicki, J. Neurocytol. 27 (1998) 707–718.
[11] A.J. Yang, D. Chandswangbhuvana, L. Margol, C.G. Glabe, J. Neurosci. Res. 52 (1998) 691–698.
[12] Y.J. Zhu, H. Lin, R. Lal, FASEB J. 14 (2000) 1244–1254.

[13] J.Y.A. Lehtonen, J.M. Holopainen, P.K.J. Kinnunen, Biochemistry (USA) 35 (1996) 9407–9414.
[14] I.N. Singh, G. Sorrentino, J.N. Kanfer, J. Neurochem. 69 (1997) 252–258.
[15] I.N. Singh, G. Sorrentino, J.N. Kanfer, Neurochem. Res. 23 (1998) 1225–1232.
[16] N.V. Koudinova, A.R. Koudinov, E. Yavin, Neurochem. Res. 25 (2000) 653–660.
[17] J. McLaurin, A. Chakrabartty, J. Biol. Chem. 271 (1996) 26482–26489.
[18] K. Matsuzaki, Ch. Horikiri, Biochemistry (USA) 38 (1999) 4137–4142.
[19] J. Vargas, J.M. Alarcon, E. Rojas, Biophys. J. 79 (2000) 934–944.
[20] T. Pillot, M. Goethals, B. Vanloo, C. Talussot, R. Brasseur, J. Vandekerckhove, M. Rosseneu, J. Biol. Chem. 271 (1996) 28757–28765.
[21] Y. Hirakura, M.C. Lin, B.L. Kagan, J. Neurosci. Res. 58 (1999) 726.
[22] H. Lin, R. Bhatia, R. Lal, FASEB J. 15 (2001) 2433–2444.
[23] N.A. Avdulov, S.V. Chochina, U. Igbavboa, E.O. O'Hare, F. Schroeder, J.P. Cleary, W.G. Wood, J. Neurochem. 68 (1997) 2086–2091.
[24] W.E. Muller, S. Koch, K. Scheuer, A. Rostock, R. Bartsch, Biochem. Pharmacol. 53 (1997) 135–140.
[25] W.E. Muller, G.P. Eckert, K. Scheuer, N.J. Cairns, A. Maras, W.F. Gattaz, Amyloid Int. J. Exp. Clin. Invest. 5 (1998) 10–15.
[26] R.P. Mason, R.F. Jacob, M.F. Walter, P.E. Mason, N.A. Avdulov, S.V. Chochina, U. Igbavboa, W.G. Wood, J. Biol. Chem. 274 (1999) 18801–18807.
[27] J.J. Kremer, M.M. Pallitto, D.J. Sklansky, R.M. Murphy, Biochemistry (USA) 39 (2000) 10309–10318.
[28] K. Halverson, P.E. Fraser, D.A. Kirschner, P.T. Lansbury, Biochemistry (USA) 29 (1990) 2639–2644.
[29] P.T. Lansbury, P.R. Costa, J.M. Griffiths, E.J. Simon, M. Auger, K.J. Halverson, D.A. Kocisko, Z.S. Hendsch, R.G. Griffin, Nat. Struct. Biol. 2 (1995) 990–998.
[30] R. Brasseur, Mol. Membr. Biol. 17 (2000) 31–40.
[31] M.I. Turan, E. Eralp, I. Ahmed, A. Kunitz, K. Itil, Psychopharmacol. Bull. 34 (1998) 391–397.
[32] B. Croisile, M. Trillet, J. Fondarai, B. Laurent, F. Mauguiere, M. Billardon, Neurology 43 (1993) 301–305.
[33] M. Tsolaki, T. Pantazi, A. Kazis, J. Intern. Med. Res. 29 (2001) 28–36.
[34] M. Rainer, H.A.M. Mucke, C. Kruger-Rainer, E. Kraxberger, M. Haushofer, K.A. Jellinger, J. Neural Transm. 108 (2001) 1327–1333.
[35] W.T. Norton, T. Abe, S.E. Poduslo, G.H. DeVries, J. Neurosci. Res. 1 (1975) 57–75.
[36] G.R. Bartlett, J. Biol. Chem. 234 (1959) 466–468.
[37] D. Hoekstra, T. De Boer, K. Klappe, J. Wilschut, Biochemistry (USA) 23 (1984) 5675–5681.
[38] N.A. Mazer, M.C. Carey, R.F. Kwasnick, G.B. Benedek, Biochemistry (USA) 18 (1979) 3064–3075.
[39] M.P. Mingeot-Leclercq, J. Piret, R. Brasseur, P.M. Tulkens, Biochem. Pharmacol. 40 (1990) 489–497.
[40] J.N. Weinstein, S. Yoshikami, P. Henkart, R. Blumenthal, W.A. Hagins, Science 195 (1977) 489.
[41] P.I. Lelkes, in: G. Gregoriadis (Ed.), Liposome Technology, CRC Press, Boca Raton, FL, 1984, pp. 225–246.
[42] S.C. Jao, K. Ma, J. Talafous, R. Orlando, M.G. Zagorski, Int. J. Exp. Clin. Invest. 4 (1997) 240–252.
[43] C.R. Sanders, G.C. Landis, Biochemistry (USA) 34 (1995) 4030–4040.
[44] J. Kyte, R.F. Doolittle, J. Mol. Biol. 157 (1982) 105–132.
[45] D. Eisenberg, R. Weiss, T. Terwilliger, Nature 299 (1982) 371–374.
[46] J.H. Davis, K.R. Jeffrey, M. Bloom, M.I. Valic, Chem. Phys. Lett. 42 (1976) 390–394.
[47] R. Brasseur, in: R. Brasseur (Ed.), Molecular Description of Biological Membranes by Computer Aided Conformational Analysis, vols. I and II, CRC Press, Boca Raton, FL, 1990.
[48] R. Brasseur, J. Biol. Chem. 266 (1991) 16120–16127.
[49] J. Peuvot, A. Schanck, M. Deleers, R. Brasseur, Biochem. Pharmacol. 50 (1995) 1129–1134.
[50] J.L. De Coen, E. Ralston, in: H. Nasvada (Ed.), Peptides, North Holland, Amsterdam, 1973, pp. 335–342.
[51] L. Lins, R. Brasseur, M. Depauw, J.P. Vanbiervliet, J.M. Ruysschaert, M. Rosseneu, B. Vanloo, Biochem. Biophys. Acta 1258 (1995) 10–18.
[52] I. Martin, M.C. Dubois, T. Defrise-Quertain, A. Saermark, A. Burny, R. Brasseur, J.M. Ruysschaert, Virology 68 (1994) 1139–1148.
[53] F. Van Bambeke, M.P. Mingeot-Leclercq, A. Schanck, R. Brasseur, P.M. Tulkens, Eur. J. Pharmacol. 247 (1993) 155–168.
[54] C.E. Dempsey, Biochim. Biophys. Acta 1031 (1990) 143–161.
[55] C.R. Sanders, J.P. Schwonek, Biochemistry (USA) 31 (1992) 8898–8905.
[56] S. Shorvon, Lancet 358 (2001) 1885–1892.
[57] J.G. Gobert, E.L. Baltes, Farmaco Pratique 32 (1977) 83–91.
[58] G. Hitzenberger, H. Rameis, C. Manigley, CNS Drugs 9 (Suppl. 1) (1998) 19–27.
[59] E.K. Gini, J. Sonnet, J. Clin. Pathol. 40 (1987) 99–102.
[60] J.M. Orgogozo, Pharmacopsychiatry 32 (Suppl. 1) (1999) 25–32.
[61] B. Van Vleymen, M. Van Zandijcke, Acta Neurol. Belg. 96 (1996) 270–280.
[62] P. Seubert, C. Vigo-Pelfrey, C. Esch, F. Lee, M. Dovey, H. Davis, D. Sinha, S. Schlossmacher, C. Swindlehurst, Nature 359 (1992) 325–327.
[63] S.R. Ji, Y. Wu, S.-F. Sui, J. Med. Chem. 277 (2002) 6273–6279.
[64] R.H. Christie, H. Chung, H. Rebeck, G.W. Strickland, B.T. Hyma, J. Neuropathol. Exp. Neurol. 55 (1996) 491–498.
[65] T. Waegemans, C.R. Wilsher, A. Danniau, S.H. Ferris, A. Kurz, B. Winblad, Dement. Geriartr. Cogn. Disord. 13 (2002) 217–224.
[66] D.J. Selkoe, Annu. Rev. Cell Biol. 10 (1994) 373–403.
[67] M. Horth, B. Lambrecht, M. Chuah Lay Khim, F. Bex, C. Clothilde, J.-M. Ruysschaert, A. Burny, R. Brasseur, EMBO J. 10 (1991) 2747–2755.
[68] M.P. Mingeot-Leclercq, L. Lins, M. Bensliman, F. Van Bambeke, P. Van der Smissen, J. Peuvot, A. Schanck, R. Brasseur, Chem. Phys. Lipids 120 (2002) 57–74.
[69] P.L. Yeagle, R.M. Epand, C.D. Richardson, T.D. Flanagan, Biochim. Biophys. Acta 1065 (1991) 49–53.
[70] R.F. Epand, J. Cheetham, P.L. Yeagle, C.D. Richardson, W.F. DeGrado, Biopolymers 32 (1992) 309–314.
[71] A. Schanck, R. Brasseur, J. Peuvot, J. Chim. Phys. 95 (1998) 467–473.
[72] A. Schanck, J. Peuvot, R. Brasseur, Biochem. Biophys. Res. Commun. 250 (1998) 12–14.
[73] J.A. Losonczi, J.H. Prestegard, J. Biomol. NMR 12 (1998) 447–451.
[74] J.A. Whiles, R. Brasseur, K.J. Glover, G. Melacini, E.A. Komives, R.R. Vold, Biophys. J. 80 (2001) 280–293.
[75] L. Lins, B. Charloteaux, A. Thomas, R. Brasseur, Proteins: Struct., Funct., Genet. 44 (2001) 435–447.
[76] S.R. Hughes, S. Goyal, J.E. Sun, P. Gonzalez-De Whitt, M.A. Fortes, N.G. Riedel, S.R. Sahasrabudhe, Proc. Natl. Acad. Sci. U. S. A. 93 (1996) 2065–2070.
[77] F.L. Festy, L. Lins, G. Peranzi, J.N. Octave, R. Brasseur, A. Thomas, Biochim. Biophys. Acta 1546 (2001) 356–364.
[78] R.F. Epand, L. Moroder, J. Lutz, T.D. Flanagan, S. Nir, R.M. Epand, Biochem. Biophys. Acta 1327 (1997) 259–268.
[79] R.P. Rand, Annu. Rev. Biophys. Bioeng. 10 (1981) 277–314.
[80] K. Klappe, J. Wilschut, S. Nir, D. Hoekstra, Biochemistry (USA) 25 (1986) 8252–8260.
[81] S. Nir, K. Klappe, D. Hoekstra, Biochemistry (USA) 25 (1986) 8261–8266.
[82] L. Chernomordik, Chem. Phys. Lipids 81 (1996) 203–213.